

Bogus dust screens from well mixed exponential disks in galaxies

Bruce G. Elmegreen¹ and David L. Block²

¹ *IBM Research Division, T.J. Watson Research Center, P.O. Box 218, Yorktown Heights, NY 10598*

² *Department of Computational and Applied Mathematics, University of the Witwatersrand, Private Bag 3, WITS 2050, South Africa*

Accepted ...; Received ...; in original form ...

ABSTRACT

The V-K colours along the minor axes of spiral galaxies typically change from red to blue with increasing distance, giving the impression that the near side is systematically screened by dust. Such a preferred orientation for dust screens is unlikely. Here we show that common extinction from the embedded dust layer in an exponential disk has the same effect, making the near side systematically redder as the inclination increases. The galaxy NGC 2841 is modelled as an example, where the V-K profile is profoundly asymmetric and actually step-like across the centre. We predict that the minor axis emission profile of the same dust in the far-infrared, at wavelength $\lambda \sim 200\mu\text{m}$, will be much more symmetric than the optical profiles, implying nearly equal column densities of dust on both sides of the minor axis.

Key words: galaxies: spiral – galaxies: ISM – galaxies: fundamental parameters – ISM: dust, extinction – infrared: galaxies – galaxies: individual: NGC 2841

1 INTRODUCTION

The recent development of K'-band ($2.1\ \mu\text{m}$) and K-band ($2.2\ \mu\text{m}$) imagery for nearby galaxy disks led to the unexpected discovery of large V-K' and V-K colour gradients along the minor axes when the inclinations exceed $\sim 60^\circ$. The ‘Evil Eye’ Galaxy NGC 4826 exhibits a sudden increase by ~ 1 magnitude from V-K=4 mag. to V-K=5 mag. in the dust attenuated ‘screen’ (Block et al. 1994a). Similarly large V-K jumps are in other highly inclined spirals, such as NGC 3521 (Panel 188 in Sandage & Bedke 1994). Explanations for this effect vary from an intervening dust screen (Witt et al. 1994) to high latitude scattering from dust (Block et al. 1996). The problem with the screen model is that the apparent dust is always on the near side of the galaxy, even though we expect random orientations for galaxies in space. The problem with the high latitude dust model is that there is no ubiquitous evidence for such dust, although extraplanar dust in specific examples has been detected (eg. Howk & Savage 1997).

This paper shows how absorption and scattering at V and K bands by dust embedded in an exponential disk can produce observed colour gradients which may be remarkably asymmetric or even step-like. The reason is that the near side of an exponential disk is brighter at smaller radius behind the dust in the midplane, while the far side is brighter at smaller radius in front of the dust in the midplane. Thus the near side has a higher fraction of the same total light blocked by dust.

Other models have considered similar effects. Kodaira & Ohta (1994) and Ohta & Kodaira (1995) measured and modelled V and J band differential extinction profiles ($= -\ln[I_{far}/I_{near}]$) along the minor axes in several galaxies, without including scattered light; they did not discuss colour gradients specifically, although the existence of such gradients can be inferred from their analyses. Byun, Freeman & Kylafis (1994) considered B and I band minor axis profiles with scattering included, but also did not specifically address the resulting near-far colour differentials (although again they can be inferred from their separate B and I profiles). Kuchinski & Terndrup (1996) plotted J-K colour profiles along the minor axes of several galaxies, but discussed and modelled only the spherical bulge systems, including scattered light. Here we determine the line-of-sight V-K colour gradient in disk+bulge galaxies using radiative transfer with direct and single-scattered light.

2 MODELS

Stellar and gaseous disks are modelled with exponential brightness and density profiles in both the radial and perpendicular directions, following the work of others referenced above. For the stellar volume emissivity, we use

$$j(r, z) = \exp\left(-r - \frac{|z|}{z_s}\right) + \frac{\epsilon_b}{(1 - R^2/R_b^2)^{1.5}}, \quad (1)$$

and for the dust extinction (scattering + absorption),

$$\kappa_\lambda(r, z) = \kappa_{\lambda,D}(0, 0) \exp\left(-r - \frac{|z|}{z_g}\right) + \frac{\kappa_{\lambda,B}(0, 0)}{(1 - R^2/R_b^2)^{1.5}}. \quad (2)$$

All distances are normalized to the disk scale length; r is the distance to a point measured parallel to the disk, R is the total galactocentric distance, in three dimensions. The volume emissivity is normalized to unity for each wavelength because we are concerned primarily with differential (near-far side) colour gradients. The intrinsic stellar colours do not matter as long as they are the same at each radius on the near and far side of the disk. Radial colour gradients in the disk do not matter for a near-far comparison either.

The equation of radiative transfer gives the intensity I measured by an observer outside the galaxy at wavelength λ :

$$I_\lambda(i) = \int_{x_0}^{x_1} dx (j[r, z] + j_{scat}[r, z]) \times \exp\left(-\int_{x_0}^x \kappa_\lambda[r, z] dx'\right). \quad (3)$$

The distance along the line of sight is x , increasing away from the observer; x_0 and x_1 are the near and far limits of the integral through the galaxy, taken here to be the hypotenuse of a triangle with a maximum total in-plane radial extent of 5 scale lengths and a maximum total half-thickness of 3 scale lengths. The argument of I_λ , i , is the galaxy inclination.

The volume emissivity from single scattering is

$$j_{scat}(r, z) = \kappa_\lambda(r, z) A_\lambda \int_{-\pi}^{\pi} dl \int_{-\pi/2}^{\pi/2} db \cos b \phi(\theta) \times \int_0^{x_2} j(r, z) d\xi \exp\left(-\int_0^\xi \kappa_\lambda[r, z] d\xi'\right). \quad (4)$$

where x_2 is the maximum distance along a path through the galaxy, l and b are the galactic longitude and latitude as seen by an observer at point x in the integral for I_λ . ϕ is the scattering phase function (Heney & Greenstein 1941),

$$\phi(\theta) = \frac{1}{4\pi} \frac{1 - g^2}{(1 + g^2 - 2g \cos \theta)^{1.5}} \quad (5)$$

and θ is the scattering angle, given by

$$\cos \theta = -\sin b \cos i + \cos b \sin i \cos l. \quad (6)$$

In equation (4), A_λ is the albedo at wavelength λ . While most interstellar grains were thought to be substantially smaller than near-infrared wavelengths (Mathis, Rumble & Nordsieck 1977), the upper size limit of dust grains – to which the near-infrared albedo is extremely sensitive – has been revised (see Kim, Martin & Hendry 1994). The first extragalactic determination of the near-infrared dust albedo was made by Witt et al. (1994), who concluded that the albedo of dust grains at V and K may be identical. This high near-infrared albedo is alluded to by a number of diverse observations (Lehtinen & Mattila 1996 for the Thumbprint Nebula; Block 1996 for the Whirlpool Galaxy M51 and its companion; Pendleton, Tielens & Werner 1990 and Sellgren, Werner & Dinerstein 1992 for infrared and classical reflection nebulae). We choose values for the optical and near-infrared albedos of dust grains to both be $A = 0.6$ in the V and K passbands.

Furthermore, dust grains are predominantly forward scattering in the optical (eg. Whittet 1992) while near-

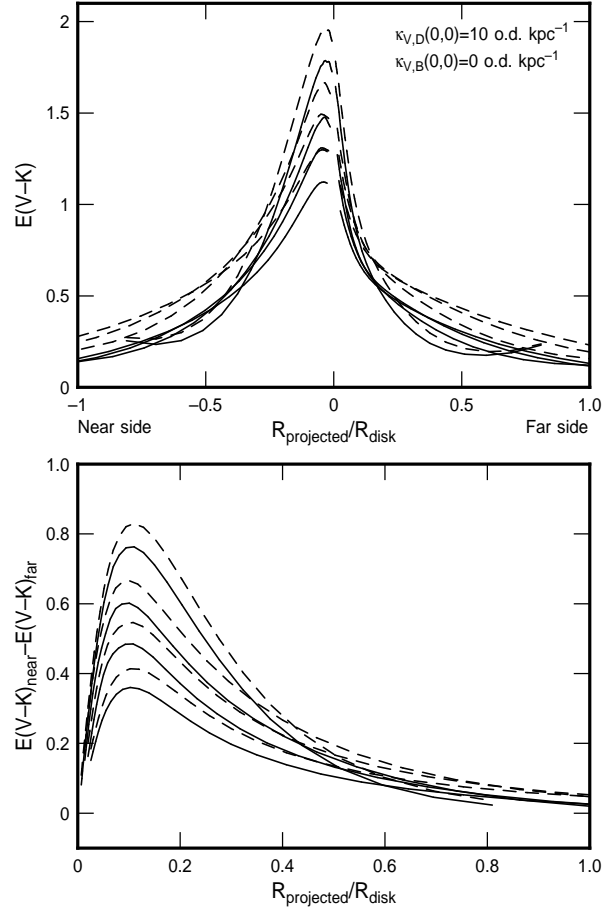


Figure 1. (top) V-K colour excess profiles along the minor axes of model galaxies with inclinations of 50° , 60° , 70° , and 80° ($E[V - K]$ increases with inclination). Solid lines include scattered light. This case has no dust distributed in the bulge. (bottom) V-K colour excess differences between the near and far sides shown as functions of minor axis distance.

infrared values of g at K lie between 0.1 and 0.6 (Witt et al. 1996). We choose $g = 0.5$ in V and K. There is only a weak dependence on g as far as albedo determinations are concerned (Fig 2 in Witt et al. 1996), and our models with different values of A did not change much; lower A gave about the same results as slightly higher extinctions, approaching the results with no scattering, as shown in the figures by dashed lines.

The intensity I_λ was determined from these equations as a function of distance from the galactic center for various galaxy inclinations. For each distance and inclination, the reddening difference between the near and far sides of the disk was evaluated in magnitudes:

$$E(V - K)_{\text{near}} - E(V - K)_{\text{far}} = -2.5 \log_{10} \left(\frac{I_V}{I_K} \right)_{\text{near}} + 2.5 \log_{10} \left(\frac{I_V}{I_K} \right)_{\text{far}}. \quad (8)$$

For most of the models shown here, the perpendicular scale heights are taken to be $z_g = 0.1$ and $z_s = 0.2$, and the bulge scale length is $R_b = 0.1$ (Kodaira, & Ohta 1994). The relative volume emissivity of the bulge is $\epsilon_b \sim 0.5 (L_b/L_d) z_s/R_b^3$ (Kodaira & Ohta 1994). The ra-

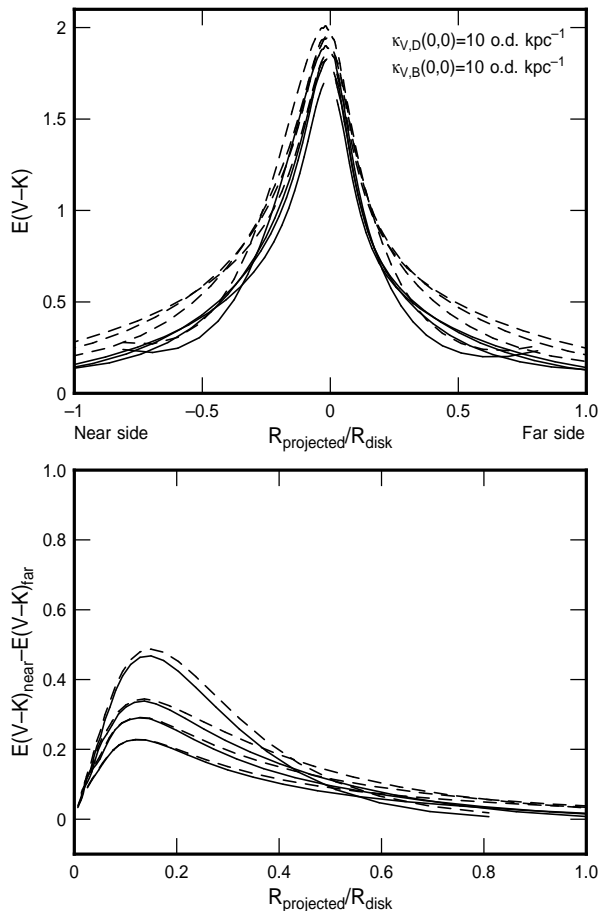


Figure 2. Same models as in the previous figure, but with dust distributed throughout the bulge region, in three-dimensions.

tio of bulge to disk luminosity is $L_b/L_d = 0.1$ at K band (Byun, Freeman & Kylafis 1994) and $0.1 \times 10^{-0.4\Delta M}$ at V band for colour difference $\Delta M = 0.5$ mag between the bulge and the disk. The central extinctions for the disk are taken to be $\kappa_{V,D}(0,0) = 10$ or 15 optical depths (o.d.) kpc^{-1} for the models shown by the figures, and for the bulge are $\kappa_{V,B}(0,0) = 0$, or 10 o.d. kpc^{-1} (1 optical depth = $0.4/\log e = 0.92$ magnitude.) In all cases, $\kappa_K = 0.1\kappa_V$. The value of $\kappa_{V,D}(0,0) = 10$ o.d. kpc^{-1} might be appropriate for the Milky Way: it gives a V-band extinction of 1.25 mag kpc^{-1} at $r = 2$ disk scale lengths, which is about the extinction at the solar radius. Many other values for these quantities were modelled too, and some of the results will be discussed for comparison.

Figure 1(top) shows the intensity versus distance along the minor axis for a model with a central disk extinction of 10 o.d. kpc^{-1} in V and no additional extinction in the bulge. The projected distance along the minor axis, $x \cos i$, is on the abscissa, in units of the intrinsic disk scale length; negative values of this distance represent the near side of the galaxy. Both the bulge and disk emissions are included here, but there is no bulge extinction in this model. Cases with scattered light are shown by solid lines, and cases without scattered light are shown by dashed lines. Inclinations of 50° , 60° , 70° , and 80° are plotted; the near-side reddening

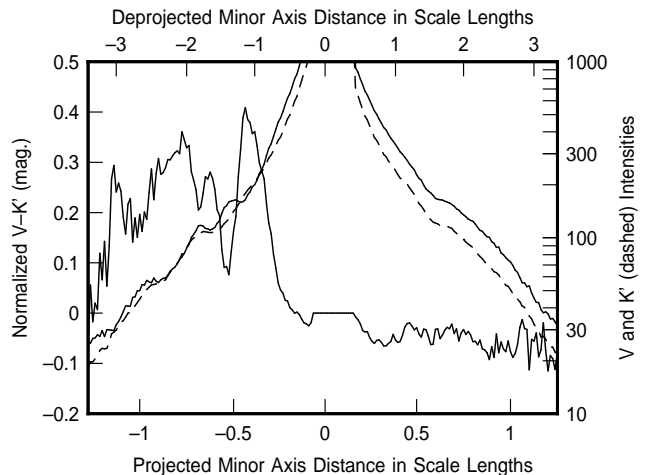


Figure 3. Minor axis V-K' profile for the galaxy NGC 2841, showing redder colours on the near side (left) than the far side. The axis for the colour difference is on the left. Also shown are the V and K' intensity scans across the minor axis, using the axis on the right. The dashed line is K'.

increases with inclination. Any intrinsic disk colour gradient that might be present in the stars is ignored.

The V-K colour differences between the near and the far sides are shown in the bottom panel of figure 1. There is a maximum in differential reddening at about 0.2 disk scale length, where the visual extinction is ~ 8 o.d. kpc^{-1} . Intrinsic disk colour gradients would not matter for this diagram, as long as the near and far sides of the disk have the same intrinsic colours at the same radii.

Figure 2 shows the same model as figure 1 but with extinction in the bulge. For the assumed central bulge extinction of $\kappa_{V,B}(0,0) = 10$ o.d. kpc^{-1} , the extinction at a radius of 1 disk scale length is 10 o.d. $\text{kpc}^{-1} (1 + [1/0.1]^2)^{-3/2} = 0.01$ mag kpc^{-1} , which is much smaller than the disk extinction at this radius. Nevertheless, dust in the bulge clearly reddens the far side of the V-K colour profile, making the V-K colour difference at the bottom of the figure about a factor of 2 less than in figure 1.

Figure 3 shows the observed V-K' scan along the minor axis of the inclined flocculent galaxy NGC 2841 (studied in more detail by Block et al. 1996). The strong colour gradient between the near (left in the figure) and far sides is evident, as discussed in our previous paper. The models in figures 1 and 2 do not reproduce this gradient well because NGC 2841 has a central hole in molecular gas inside 1 disk scale length (Young & Scoville 1982), and it has a low HI column density there too. Thus there is probably a dust hole inside 1 scale length. This hole was also evident in a scan of V-K colour versus distance along the major axis of NGC 2841 (Block et al. 1996), which shows a dip toward bluer colour inside 1 disk scale length. This blueness approaches the true colour of the inner disk, without extinction. In addition to the dust hole, NGC 2841 also has a relatively high extinction perpendicular to the disk compared to the Milky Way (Block et al. 1996), so we need to consider slightly larger κ than in the previous figures.

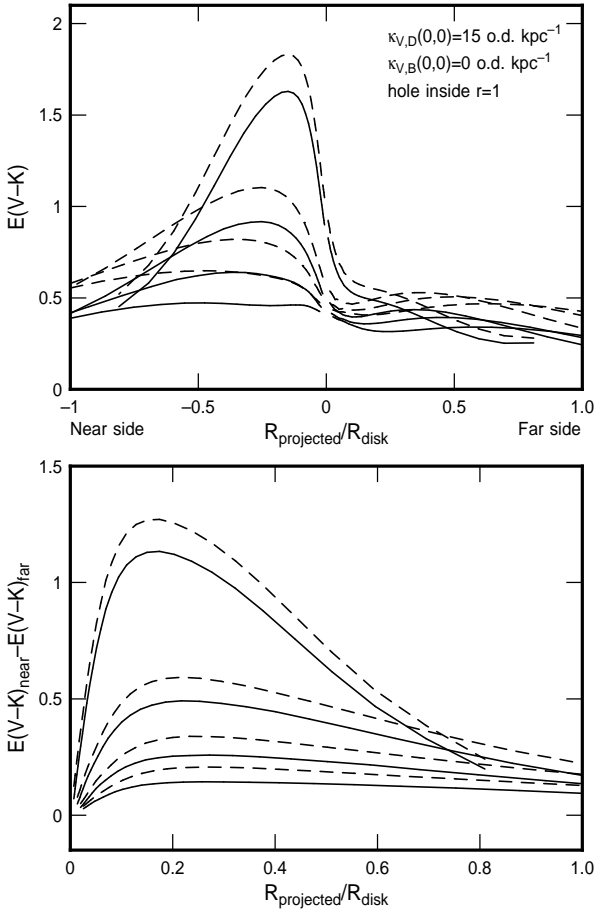


Figure 4. Model appropriate for NGC 2841 with four inclinations i as before. In this case the inclination $i = 70^\circ$, which is the second from the top, most closely matches the inclination of NGC 2841.

Figure 4 shows the minor axis profile from a model with 1.5 times the extinction as in figure 1 but with a central hole made by setting the dust density profile equal to re^{-r} instead of e^{-r} for radius r , measured in units of the scale length. This function gives a peak in the gas density at $r = 1$ with a hole inside this and a nearly exponential disk beyond. The model has the same four inclination angles as in the previous plots, for general use in other studies; the inclination of NGC 2841 is $\sim 68^\circ$, which is essentially the same as for the third curve up from the bottom (which is for 70°). With a hole in the model and no dust in the bulge, the fit to the data is good, i.e., the near side is redder than the far side by ~ 0.4 mag., and the far side colour excess distribution is relatively flat. The small scale variations in the data for NGC 2841 are presumably from dust lanes, which are not part of the present model (but see Block et al. 1996 for radiative transfer fits to these dust lanes).

Figure 5 shows the same disk-hole model as in figure 4, but with extinction in the bulge as in figure 2. This model does not fit the data for NGC 2841 because the far side is too red with the additional extinction from the bulge, giving the far-side part of the curve on the top of figure 5 a downward slope, unlike the observations of NGC 2841 and the corresponding curve in figure 4, where this far-side $E(V-$

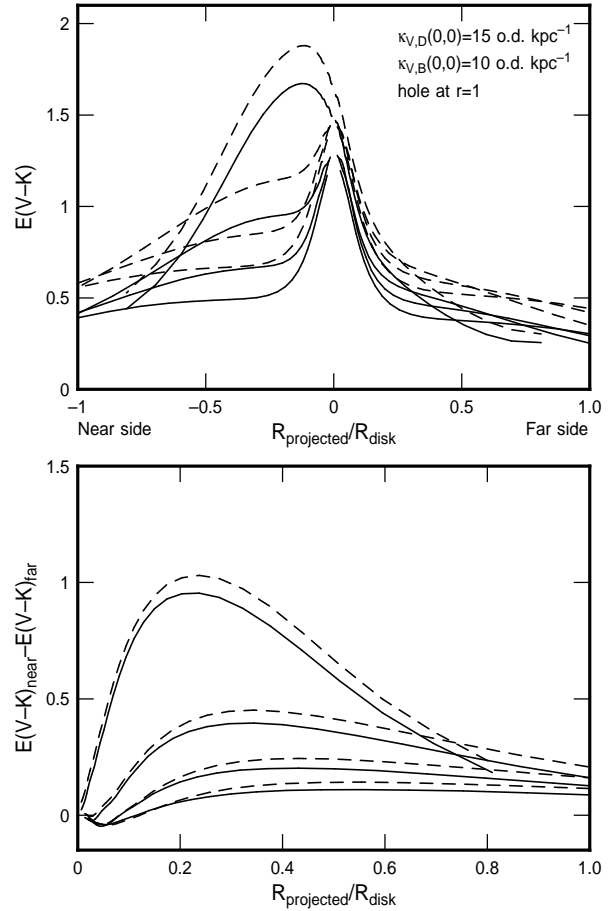


Figure 5. Model with a disk dust distribution as in Fig. 4, but with dust also in the bulge, off the plane. This case is not a good match for NGC 2841 because the bulge dust reddens the far side of the disk, and produces too high a colour differential there.

K) scan is flat. The dusty-bulge model also has an increased reddening in the central region, which becomes even more prominent for face-on orientations. Any larger $K_{V,B}(0,0)$ makes this central reddening unacceptably large even for the inclination of NGC 2841. Thus the upper limit to the amount of bulge dust in NGC 2841 is about the value in figure 5, which corresponds to less than 0.01 o.d. kpc^{-1} at one scale length, or an equivalent hydrogen density of < 0.007 cm^{-3} , using the standard conversion of dust to gas (Bohlin, Savage & Drake 1978). Evidently our previous suggestion (Block et al. 1996) that the near-far colour difference in NGC 2841 is the result of bulge scattering by dust high off the plane is not correct.

The variable geometry of dust and starlight along the line of sight makes the relationship between color excess and extinction non-linear, unlike the common interstellar case where an absorbing cloud is in front of a single star. Figure 6 plots the reddening versus the optical depth through the disk for the Milky Way and NGC 2841 models with no bulge dust (from Figs. 1 and 4) and with scattered light included. The projected radius along the minor axis varies along each curve, from the near side of the disk (solid line) to the far side (dashed line). The same four inclination an-

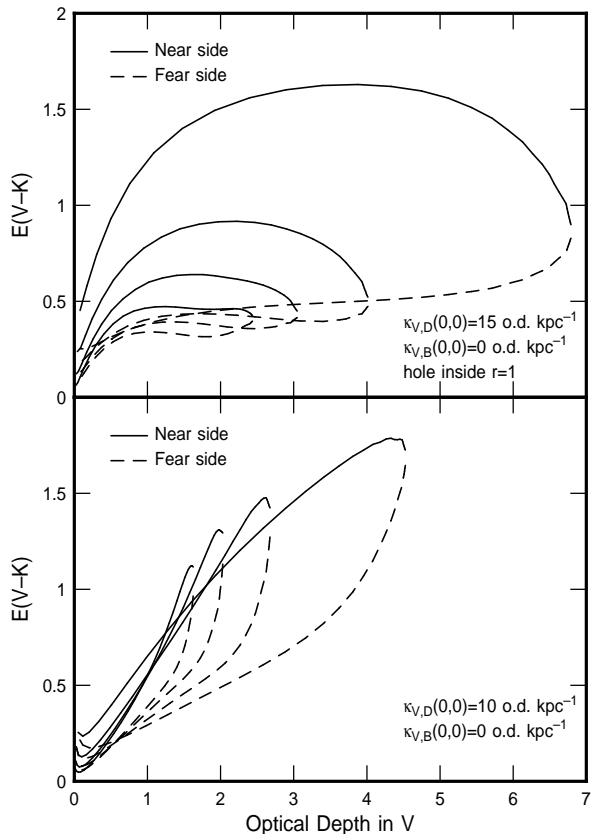


Figure 6. Color excess versus optical depth through the disk for the Milky Way and NGC 2841 models shown previously in figures 1 and 4. The lack of a simple linear relationship results from the varying distribution of dust and starlight on the line of sight.

gles are shown. The relationship between reddening and extinction is double-valued because the near side has more reddening per unit dust column density than the far side.

3 DISCUSSION

Differential reddening between the near and far sides of a galaxy disk may be understood as follows: The radial light gradients in the bulge and disk cause the near side to have a brighter light source *behind* most of the disk dust, while the same gradients on the far side cause it to have its brighter light source in *front* of the disk dust. Thus the disk dust has more light to block on the near side than the far side. Consequently the near side is dimmer (Kodaira & Ohta 1994; Byun, Freeman, & Kylafis 1994) and significantly redder. Models with the same scale height for the dust and stars (not shown) have even stronger colour differentials because more of the starlight is extinguished. Models with more disk extinction also have more differential reddening, and models with dust in the bulge have less because the bulge dust makes the far side redder.

Minor axis colour gradients are present in many of the galaxies in Wray’s Color Atlas (1988) and are even more prominent in $V - K$ images of inclined galaxies (e.g., see Peletier and Balcells 1997; Thornley 1996 & 1997; Grosbøl

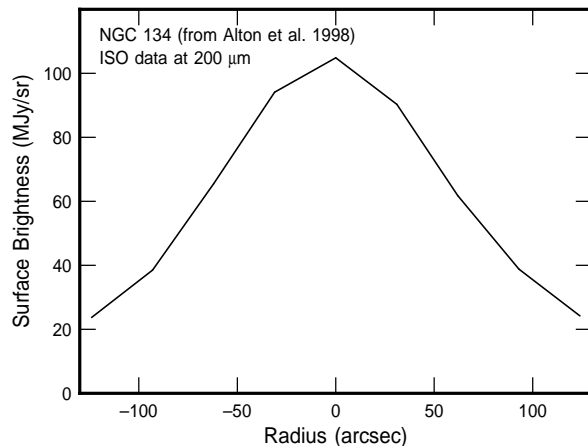


Figure 7. Surface brightness along the minor axis of the galaxy NGC 134 at $200 \mu\text{m}$, from Alton et al. (1998), showing symmetry in cold dust emission even though this same dust presents a striking asymmetry with foreground “screening” in optical images.

& Patsis 1998; Block et al. 1994a). Thornley (1996) found that in NGC 5055, optical depths suddenly jump from 0.5 on the far side, to 4–5 on the near side.

The models presented here show that such colour gradients are a natural result of extinction from well mixed dust embedded in the disk, and it is predicted that for large enough inclinations, particularly in galaxies with inner-disk dust holes, the near-far asymmetry in $V-K$ profiles may even be step like. Near-side dust screens are not needed, even for the dramatic jump of $E(V - K) \sim 1$ mag in NGC 4826. There is some sensitivity of the colour gradient to the precise distribution of dust, such as the presence or lack of a central hole, and this may be useful in modelling disks.

Another point to stress is that the far side, although bluer, cannot be considered *dust free* or *unobscured* – terms that continue to be used in the literature. For example, the Andromeda spiral M31 shows prominent dust lanes on the far side as well as the near side in both the IRAS $60 \mu\text{m}$ and $100 \mu\text{m}$ maps (eg. Habing et al. 1984; Walterbos & Schwering 1987). NGC 2841 also has arms of dust in K' images on both sides (Fig 1c in Block et al. 1996 and plate 3 in Block 1996), as does M51 at $15 \mu\text{m}$ (Sauvage et al. 1996, Block et al. 1997). It is simply that when the disk is well inclined to the line of sight, the near-side dust appears to be much thicker than the far side dust, even when both the dust and the stellar column densities are the same on each side.

These results lead to a prediction about the *emission* from cold ($T \sim 20\text{K}$) galactic dust: the far-infrared minor axis luminosity profile across a galaxy, at wavelengths of $\sim 180 \mu\text{m}$ or longer, should be *symmetric*, even if the optical profile is so asymmetric that it appears to be screened by dust on one side. That is, optically screened galaxies will be found to have nearly equal column densities of cold dust on both sides of the minor axis.

A good example is NGC 134, which was cited by Sandage & Bedke (1994) as displaying a “particularly strong” dust asymmetry between the near and far sides (see Panel 194 in their Atlas). This galaxy has just been observed at $200 \mu\text{m}$ (Alton et al. 1998) by the Infrared Space

Observatory. The far-infrared emission profile of NGC 134, shown in figure 7, is in fact almost perfectly symmetric across the minor axis (Alton, private communication). Thus equal amounts of cold dust, which accounts for $\sim 90\%$ of the dust mass (Block 1996; Block et al. 1994a), reside on either side of the minor axis, despite its apparently striking foreground dust screen.

Another implication of the model results, illustrated by figure 6, is that galactic opacity is not simply related to color excess. The conversion from color excess to opacity depends on inclination and position in the disk. For galaxies well inclined to the line of sight, there are many E(V-K) values for the *same* optical depth, with extrema on the minor axes and intermediate values elsewhere. If this is not taken into account, one might erroneously find, on the basis of E(V-K) colour excesses, that the bluer far side contains less dust than the redder near side – and will incorrectly compute differences in the dust masses of the near and far sides – although both sides contain equal amounts. Figure 6 does suggest, however, that the *average* of the color excesses for the near and far sides might have some simple relation to the opacity at that radius when there is no inner hole. From the bottom panel of this figure, we obtain $\tau \sim 2.5(E[V - K]_{near} + E[V - K]_{far})/2$. Converting this to visual magnitudes gives $A_V \sim 2.7(E[V - K]_{near} + E[V - K]_{far})/2$. Note that this conversion factor is much larger than the conventional factor from V-K color excess to A_V , based on foreground extinction for single stars, which gives $A_V \sim 1.09E(V - K)$ (Savage & Mathis 1979; Whittet 1988). The larger factor here arises because nearly half of the dust on the line of sight is on the far side of the disk, and this dust occults relatively few galactic stars.

Our results might also have a practical application. We have noted that when a minor axis colour gradient is found, the red side should be nearer. Thus the sense of dominant rotation in a disk galaxy can be determined from the colour gradient if trailing spiral arms are present. Such determinations may be useful for crowded fields of distant galaxies in an attempt to look for alignment or other attributes of spin orientations without the tedious job of taking slit spectra to get rotation curves. This characteristic of disk colour might also be useful in searching for leading spiral arms in galaxies with rotation curves. Such arms apparently occur in some accreting galaxies (NGC 4622: Buta et al 1992, see also Fig 7 in Block et al. 1994b and plate 4 in Bertin & Lin 1996; NGC 4826: van Driel & Buta 1993).

4 ACKNOWLEDGEMENTS

The research of DLB is supported by the Anglo American and de Beers Chairman's Fund Educational Trust, and a note of great appreciation is expressed to Mrs. M. Keeton and the Board of Trustees.

REFERENCES

Alton, P.B., Trewhella, M., Davies, J.I. et al. 1998, A&A, 335, 807.
 Bertin, G., & Lin, C.C. 1996, *Spiral Structure in Galaxies – A Density Wave Theory* (MIT Press, Cambridge, Mass)

Block, D.L., Witt, A.N., Grosbøl, P., Stockton, A., & Moneti, A. 1994a, AA, 288, 383
 Block, D.L., Bertin, G., Stockton, A., Grosbøl, P., Moorwood, A.F.M., & Peletier, R.F. 1994b, AA, 288, 365
 Block, D.L., Elmegreen, B.G., & Wainscoat, R.J. 1996, Nature, 381, 674
 Block, D.L. 1996 in *New Extragalactic Perspectives in the New South Africa* (ed. Block, D.L. & Greenberg, J.M.: Kluwer Academic Press), ASSL 209, 1
 Block, D.L., Elmegreen, B.G., Stockton, A., & Sauvage, M. 1997, ApJ, 486, L95
 Bohlin, R.C., Savage, B.D. & Drake, J.F. 1978, ApJ, 224, 132
 Buta, R., Crocker, D.A., & Byrd, G.G. 1992, AJ, 103, 1526
 Byun, Y.I., Freeman, K.C., & Kylafis, N.D. 1994, ApJ, 432, 114
 Grosbøl, P.J. & Patsis, P.A. 1998, A&A, 336, 840
 Habing H.J et al. 1984, ApJ, 278, 59
 Henyey, L.G., & Greenstein, J.L. 1941, ApJ, 93, 70
 Howk, J.C., & Savage, B.D. 1997, AJ, 114, 2463
 Kim, S.-H., Martin, P.G., & Hendry, P.D. 1994, ApJ, 422, 164
 Kodaira, K., & Ohta, K. 1994, PASJ, 46, 155
 Kuchinski, L.E., & Terndrup, D.M. 1996, AJ, 111, 1073
 Lehtinen, K., & Mattila, K. 1996, AA, 309, 570
 Mathis, J.S., Rumble, W., & Nordsieck, K.H. 1977, ApJ, 217, 425
 Ohta, K., & Kodaira, K. 1995, PASJ, 47, 17
 Peletier, R.F., & Balcells, M. 1997, NewA, 1, 349
 Pendleton, Y.J., Tielens, A.G.M., & Werner, M.W. 1990, ApJ, 349, 107
 Sandage, A. & Bedke, J. 1994, *The Carnegie Atlas of Galaxies* (Carnegie Inst. of Washington)
 Sauvage, M. et al. 1996, AA, 315, L89
 Savage, B.D., & Mathis, J.S. 1979, ARAA, 17, 73
 Sellgren, K., Werner, M.W., & Dinerstein, H.L. 1983, ApJ, 271, L13
 Thornley, M.D. 1996, ApJ, 233, 56
 Thornley, M.D. 1997, PhD dissertation (Univ of Maryland, College Park, MD)
 van Driel, W., & Buta, R. 1993, PASJ, 45, 47
 Walterbos, R.A.M. & Schwering, P.B.W. 1987, AA, 180, 27
 Whittet, D.C.B. 1988 *Dust in the Universe*, ed. Bailey, M.E. & Williams, D.A., Cambridge: Cambridge Univ Press, 25.
 Whittet, D.C.B. 1992, *Dust in the Galactic Environment*, (Institute of Physics, Bristol), 69
 Witt, A.N., Lindell, R.S., Block, D.L., & Evans, R. 1994, ApJ, 427, 227
 Witt, A.N., Petersohn, J.K., Lindell, R.S., Block, D.L., & Evans, R. 1996 in *Spiral Galaxies in the Near-Infrared* (ed. D. Minniti & H. -W. Rix: Springer Verlag), 277
 Wray, J.D. 1988, *The Color Atlas of Galaxies* (Cambridge Univ. Press)
 Young, J.S., & Scoville, N. 1982, ApJ, 260, 41

This paper has been produced using the Royal Astronomical Society/Blackwell Science L^AT_EX style file.